Available online at www.sciencedirect.com
ScienceDirect
Polymer 48 (2007) 5369–5375
polymer
www.elsevier.com/locate/polymer

Gelatin–clay nanocomposites of improved properties☆

YuanQiao Rao*

Kodak Research Labs, CTO Organization, Eastman Kodak Company, Rochester, NY 14650-2109, United States

Received 30 April 2007; received in revised form 27 June 2007; accepted 28 June 2007
Available online 6 July 2007

Abstract

Transparent gelatin–clay nanocomposite films were made through solution processing. These films exhibit enhanced physical performance. The Young's modulus of the composite film was 8.3 GPa, almost three times that of gelatin alone, by dispersing only 10 wt% of one type of montmorillonite clay into the nanosized phase in the gelatin. With the addition of the clay nanoparticles, the crystallinity of gelatin decreases and the melting point increases slightly. X-ray diffraction (XRD) and transmission electron microscopy (TEM) disclosed that the clay nanoplatelets are well exfoliated and dispersed, and are parallel to the plane of film in the nanocomposite film. The property enhancements of gelatin are affected by the dispersion of particles (i.e., intercalation and exfoliation), particle properties (i.e., particle aspect ratio), and particle–matrix interaction, as studied by XRD and TEM. The property enhancement can be well modeled using the Halpin–Tsai equation.

Keyword: Clay nanocomposites; Gelatin; Property

1. Introduction

At the present time, nanocomposites are receiving a great deal of attention from materials scientists. A composite is called a nanocomposite when the dimension of at least one of its phases is less than 100 nm. It is believed that when the domain size is comparable to the size of a molecule, the atomic and molecular interactions can have a significant influence on the macroscopic properties of that material. Thus, superior property enhancements can be achieved.

One subcategory of nanocomposites is the clay nanocomposite, where nanosized clay particles are used as reinforcing media. Clay is inexpensive, chemically and thermally stable, and has good mechanical properties. Pioneer work at Toyota stimulated the research on polymer–clay nanocomposites [1–3]. The platelet-like geometry of clay makes it ideal as a property-enhancing additive. Since then, a variety of polymers have been evaluated with the addition of clay, including thermoplastics of nylon 6 [1–4], PET [5–9], nylon-MXD6 [10], polystyrene [11,12], PMMA [13], polypropylene [14], PBT [15], PC/PET blend [16], polyaniline [17], thermosets of epoxy [18], water-soluble polymers such as poly(ethylene oxide) [19–21], poly(vinylpyrrolidone) [22], polyvinyl alcohol [23], and water born polymeric latex [24]. An enhancement in the mechanical properties, an increase in the heat distortion temperature, a lowering in the gas permeability, the use as absorbents, additives for rheological controlling and antistatic material, and an improvement of flame-retardant property [25] were observed in various polymer–clay nanocomposites. However, property enhancement depends very much upon the system that is chosen. Many nanocomposite systems do not yield the same degree of property enhancement as that achieved by the polyamide clay nanocomposites [1–4]. It is assumed generally that the two factors, the opening up or intercalation, of the clay sheets, and the dispersion of the intercalated platelets, determine the change in properties. Small and wide-angle X-ray diffractions (XRD) were utilized to investigate the preferred orientation of polymer in the presence of the clay. Attenuated total reflectance Fourier transform infrared (ATR FTIR) was used to study the interaction between the clay and the polymer. A multiscale micromechanical

☆ Partially presented at 2006 Antec meeting.

* Tel.: +1 585 588 2609; fax: +1 585 477 7781.
E-mail address: yuanqiao.rao@kodak.com

0032-3861/$ - see front matter © 2007 Elsevier Ltd. All rights reserved.
doi:10.1016/j.polymer.2007.06.068

model was proposed to predict clay nanocomposite behavior [5]. The study suggested the use of effective particles in the treatment. It is the objective of this paper to explore new properties, achieve better property enhancements in clay-containing nanocomposites, and illustrate the structure–property relationship in nanocomposites.

In our study, gelatin–clay nanocomposites were produced and studied. Gelatin, a natural polymer, has been used in photographic products for many years. It has good physical properties, but it is sensitive to environmental humidity. Gelatin with enhanced tensile properties and a reduction in humidity sensitivity is desired.

2. Experimental

2.1. Materials

Two different types of clay were used in this experiment. Laponite® RDS and Cloisite® Na^+ were supplied by Southern Clay Products, Inc. (Gonzales, TX, USA). Laponite RDS is a synthetic hectorite of a fine, white powder with a reported aspect ratio (length/thickness (L/t)) of 20–30. Cloisite Na^+ is a purified, naturally occurring smectic silicate of a greenish-yellow powder with a reported aspect ratio (L/t) of 200. The gelatin used was a type 4, class 30, nondeionized gelatin (30–122), with a density of 1.34 g/cm^3.

2.2. Making a gelatin–clay nanocomposite

An aqueous mixture of a 4% solid concentration of clay and gelatin of different compositions was made in a 50 °C water bath using a high shear device. The coating was made on a clean PET film using a coating knife with 1 mm clearance. The coating was immediately cooled to 4 °C to form the desired gel structure. The coating was placed in an ambient environment to dry for at least two days. A freestanding film of approximately 25 μm was peeled from the PET substrate and stored in a standard 50% RH, 23 °C environment before further testing.

2.3. Characterization

According to the ASTM D 882-80a, tensile properties were measured. A Perkin–Elmer DSC 7 was used to conduct the calorimetric study of the gelatin–clay films. The heating rate was 10 °C/min. A dimensional stability gauge (DSG) was used to measure the dimension of the specimen at different relative humidities. The sample length at 50% RH was recorded as the original length l_0. The dimensions of samples at a series of RHs of 15, 30, 40, 50, 70, and 80% were tested, and the humidity expansion coefficient was calculated based on the following equation.

$$\mathrm{HEC} = \frac{\Delta l}{l_0 \cdot \Delta \mathrm{RH}} * 10^6 \mathrm{ppm}/\%\mathrm{RH} \quad (1)$$

The structure of the gelatin–clay nanocomposite film was characterized by XRD and transmission electron microscopy (TEM). All XRD data were collected using a Rigaku RU-300 Bragg–Brentano diffractometer coupled to a copper-rotating anode X-ray source. TEM was done using a Joel 2000 TEM.

3. Results and discussion

It is well known that process conditions have a significant influence on the physical performance [26–28] and structure [29] of gelatin solid films. Therefore, the making of the gelatin–clay nanocomposite films was well controlled to ensure the comparability among samples. The content of added clay is expressed in this paper as weight percentage (wt%), unless otherwise specified.

Gelatin is water-soluble and polyampholytic in water. Therefore, water can participate in the composite making and facilitate the intercalation of the clay sheets. Gelatin has a good electrostatic interaction with clay and can further forms hydrogen bonding. It is shown that a well-dispersed composite can be formed once the clay sheet is intercalated.

3.1. Structure characterization

It is generally believed that the intercalation of the clay sheets and the elimination of the agglomeration of clay nanofiller are important to achieve good properties in gelatin–clay composites. In the gelatin–clay composite, the water was used first to exfoliate clay sheets; then the gelatin was added to the mixture. The high shear mixing ensured a good dispersion of the nanofillers, and the presence of polymer inhibits their re-aggregation.

XRD was used to examine the morphology in the solid gelatin–clay film. Clay particles have a characteristic interlayer spacing of 9 Å of (001) plane. During mixing, this interlayer opens up. If the matrix molecule enters this interlayer space, the clay is intercalated. Eventually, the association between two clay platelets is lost, and the clay is considered to be exfoliated. In the exfoliated state, the diffraction from the clay interlayer spacing disappears, and it is believed that the two clay platelets are at least 70 Å apart. Thus far, research shows that at least an intercalated state is needed for desired property enhancement. XRD of pure clay shows a distinctive diffraction peak at a 2θ of $\sim$6.5°, corresponding to a basal spacing of $\sim$12 Å as shown in Fig. 1, trace (b). In comparison, XRD of all of the studied nanocomposite films shows no diffraction peak (Fig. 1, trace (a)), indicating that the clay is in an exfoliated state. The higher the aspect ratio of the clay, the less of it can be added to a composite and still maintain full exfoliation. For instance, when the high-aspect-ratio clay, Cloisite, is used, the gelatin–clay nanocomposite stays exfoliated up to 10%. For a low-aspect-ratio clay, such as Laponite, upon addition of clay into the composite gelatin, the clay still remains exfoliated at 25%. It was also observed that, although gelatin typically crystallizes when coated as shown in Fig. 1 trace (c), the addition of clay depresses the crystallization of the gelatin

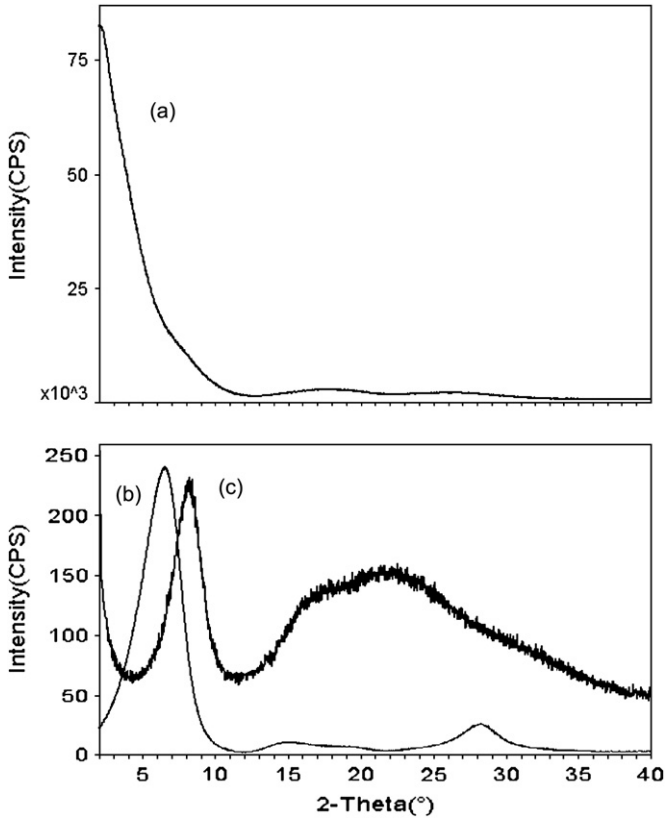

Fig. 1. XRD trace: (a) 25:75/Laponite:gelatin nanocomposite film, (b) Laponite clay and (c) gelatin.

and the diffraction peak of the gelatin crystal becomes indistinguishable. (Fig. 1, trace (a)) This is consistent with the DSC observation, which will be discussed later (Fig. 6).

The dispersion of the clay nanoplatelet was also investigated using TEM. A TEM photo, Fig. 2, of the composite shows that the clay nanoplatelets are uniformly dispersed in the gelatin matrix. It is also noted that the clay nanoplatelet assumes a preferred orientation, which is parallel to the film surface. This is in contrast to the many reported morphologies of clay–polymer nanocomposites generated from the melting process, where heterogeneous phases are often formed. The alignment of the filler is known to contribute to property enhancements in fiber or flake-filler composites.

The information gathered by combining XRD and TEM measurements confirms that the majority of clay particles are in an exfoliated state and it will be further shown that the exfoliation of the clay particle has significant impact on the properties of the composites.

3.2. Mechanical properties

Two series of gelatin–clay nanocomposites with varying clay content were prepared, using two types of clay: Cloisite Na^+ and Laponite RDS. They are called gelatin–Cloisite and gelatin–Laponite nanocomposites, respectively. The content of clay changed from 1 to 25%. All nanocomposite films

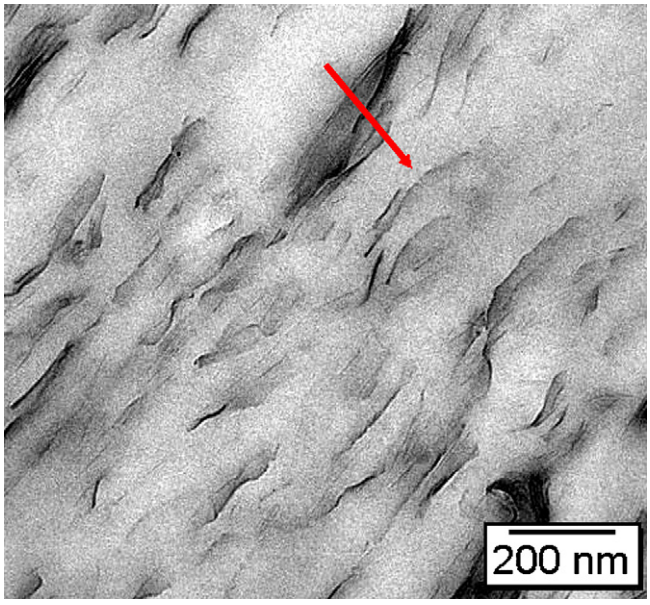

Fig. 2. TEM of gelatin–Cloisite nanocomposite film; the arrow indicates the direction of the film thickness.

are transparent in the studied clay-loading range as shown by Fig. 3.

Table 1 lists the property of the composite at different Cloisite loading levels. From our experiments, a low loading of Cloisite in gelatin yields good improvement in mechanical properties. At a loading of 5% Cloisite, the Young's modulus increased by 75%, and the tensile strength increased by 25%. Meanwhile, the break elongation decreased from 10 to 3%. The Young's modulus of the composite further increased to 8.3 GPa, which is 2.5 times that of the virgin polymer as shown in Fig. 4. A comparison between the stress–strain curves of the pure polymer and the gelatin–Cloisite nanocomposite of 5 wt% of Cloisite is shown in Fig. 5. This improvement is comparable to the clay–nylon nanocomposite and is generally better than many other polymer–clay nanocomposites [5]. Fig. 4 discloses that the Young's modulus linearly increases with the volume fraction of the added Cloisite clay. The Young's modulus changed with the volume fraction of the added clay in a linear manner. The extrapolated Young's modulus of the clay is 108 GPa. This number is close to a calculated modulus using effective particle property [30,31].

In the study of composites, the aspect ratio of the filler is found to have influence over the properties of the composites. In order to study the effect of the aspect ratio of the filler on the property of nanocomposites, another type of clay, Laponite RDS, was used. Laponite RDS has an order of magnitude lower aspect ratio than Cloisite.

Fig. 4 compares the tensile properties of a gelatin nanocomposite containing two different types of clay. Clearly, the gelatin–clay composite containing the higher aspect ratio clay particles has much higher modulus than that containing the lower aspect ratio clay at the same clay-loading content. It has been shown in the structure characterizations that both clays are at the exfoliated state. Therefore, difference in

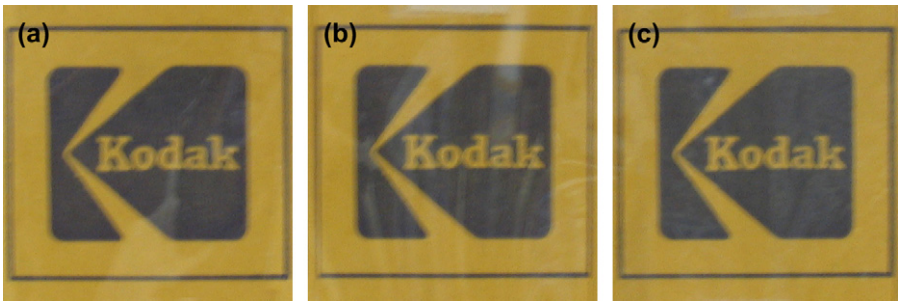

Fig. 3. The transmission of the nanocomposite films as shown putting the films of different compositions over a Kodak logo: (a) pure gelatin; (b) gelatin–Laponite of 25 wt% Laponite and (c) gelatin–Cloisite of 10 wt% Cloisite.

property enhancement is caused by the different aspect ratios of the two clays, rather than the difference in the dispersion quality of the nanofillers.

3.3. Thermal properties

To probe the interaction between the clay nanoplatelet and gelatin, a thermal study on the gelatin–clay nanocomposites is conducted. The procedure yields a gelatin film with a gel structure of 26.3 J/g (6 cal/g), T_g of 56.4 °C, and T_m of 86.6 °C.

The DSC traces of the gelatin–clay nanocomposites are shown in Fig. 6. It is observed that the melting point slightly increases with the addition of clay, while the melting enthalpy decreases. This indicates that the crystallinity is depressed by the addition of clay, which is often observed in other composite systems. At the same time, the gelatin crystal becomes more perfect and has a higher melting point. A DSC rescan of the gelatin–Cloisite of 10 wt% Cloisite was done from 25 to 200 °C after heating the nanocomposite sample to 200 °C and cooling down to 25 °C at 20 °C/min. No thermal transitions were detected in the second heating. This suggests that during the first heating, gelatin crystals are melted and the molten gelatin molecules are not able to reorganize into crystalline phase in the presence of strong interacting clay platelet upon cooling. The T_g of the gelatin–clay nanocomposites appears to be similar to that of pure gelatin.

3.4. Humidity expansion

The properties of gelatin are known to be sensitive to humidity and the dimension of a gelatin film changes significantly at different humidities. The mismatch of the humidity expansion coefficient in a multilayer structure can create large internal stresses and cause curl. It is desirable to lower the humidity expansion coefficient of the gelatin. A humidity expansion coefficient was calculated according to Eq. (1). As listed in Table 2, the humidity expansion coefficient of the gelatin–Cloisite is lower than the gelatin–Laponite, and both are lower than pure gelatin. A 5% addition of Cloisite lowers the humidity expansion coefficient of gelatin by a factor of 2.

Table 1
Mechanical properties of gelatin–Cloisite nanocomposite films

Cloisite concentration (wt%)	Young's modulus (GPa)	Maximum stress (MPa)	Break elongation (%)
0	3.3	88.9	9.6
1	3.5	88.1	8
3	4.7	97.4	3.6
5	5.9	97.4	3
10	8.3	110.8	0.9

3.5. Modulus modeling using the Halpin–Tsai equation

It is commonly believed that significant property change can happen when a phase size is close to nanometers. Although many systems and properties were studied, there is little understanding about the mechanism of property enhancement and design principle. Meanwhile, composites have existed for several decades and many studies and theories on composites were developed. It is worthwhile to examine the applicability of some composite theories on the nanocomposites. This will shed light on the possible mechanism of property enhancement and provide a basis for a further modeling effort.

Most composite theories on the moduli originated from the viscosity of suspensions. When the filled phase is comparable to the size of a molecule, the viscosity of the filled system is

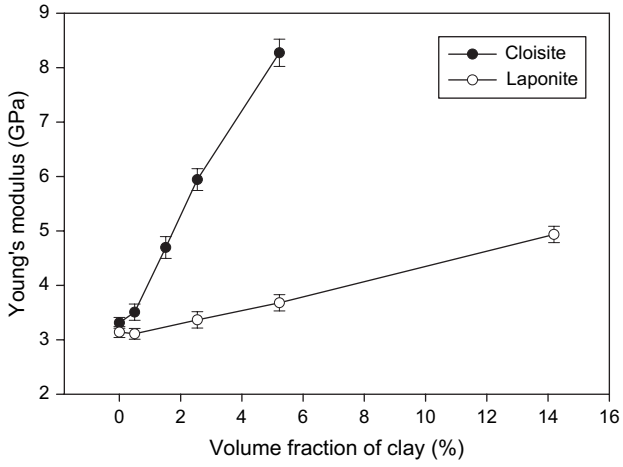

Fig. 4. Change in Young's modulus with the weight fraction of gelatin–clay nanocomposite film: solid circle: Cloisite and open circle: Laponite.

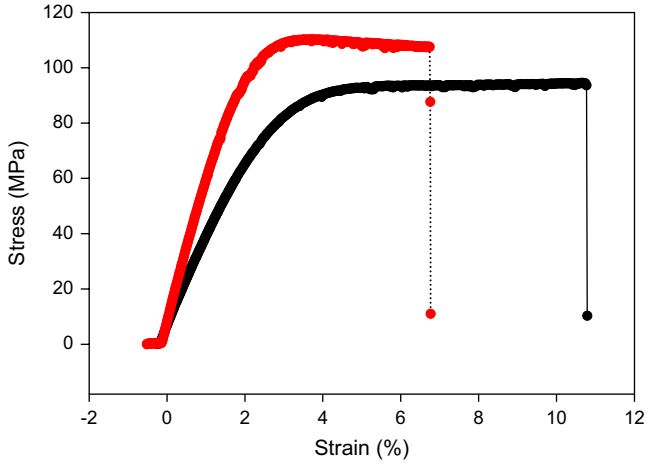

Fig. 5. Examples of stress–strain curves: red curve is a 95/5 (wt) gelatin–Cloisite composite film; and the black curve is a pure gelatin film (for interpretation of the references to colour in this figure legend, the reader is referred to the web version of this article).

expected to follow Einstein's equation at very low concentration, and more generally, the Mooney's equation at higher concentration:

$$\ln \frac{\eta}{\eta_1} = \frac{k_E \phi_2}{1 - \phi_2/\phi_m} \tag{2}$$

where η is the viscosity of the filled system, η_1 is the viscosity of the matrix, K_E is the Einstein coefficient, ϕ_2 is the volume fraction of the filled phase, ϕ_m is the maximum packing efficiency:

$$\phi_m = \frac{\text{true volume of the filler}}{\text{apparent volume occupied by the filler}} \tag{3}$$

Eq. (2) can be generalized for different moduli of the composites:

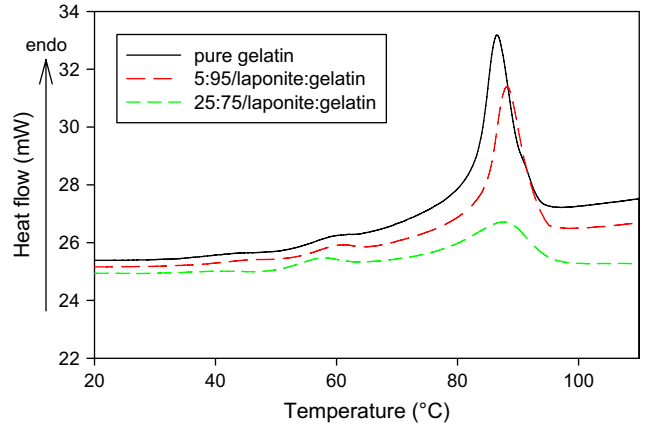

Fig. 6. DSC traces of gelatin–Laponite nanocomposite films at different Laponite contents: black solid line represents pure gelatin, red dashed line represents gel composite of 5 wt% Laponite; and green dashed line represents gel composite of 25 wt% Laponite (for interpretation of the references to colour in this figure legend, the reader is referred to the web version of this article).

Table 2
Humidity expansion coefficient of different gelatin–clay nanocomposites

Material	HEC1 (15–50 RH) (ppm/% RH)	HEC2 (50–80 RH) (ppm/% RH)
Gelatin	435.4	146.4
5:95/Laponite:gelatin	379.4	86.4
5:95/Cloisite:gelatin	262.1	81.2
10:90/Cloisite:gelatin	189.3	62.1

$$\ln \frac{P}{P_1} = \frac{k_E \phi_2}{1 - \phi_2/\phi_m} \tag{4}$$

where P is any modulus of the composite: Young's, shear or bulk.

It is shown by Eq. (2) that the properties of the composite will be largely influenced by the Einstein coefficient of the filler, which is related to the aspect ratio of the filler particle through the following equation [32]:

$$K_E = 2.5 \cdot (L/t)^{0.645} \tag{5}$$

where L is the length of the filler particle and t is the thickness. It is predicted from the Mooney equation that the higher the aspect ratio, the larger the moduli enhancement.

However, the Mooney equation often predicts far too high moduli for composites. When the modulus ratio of the filler and the matrix is not infinite, the deformation contribution from the rigid phase needs to be considered. A more complete treatment was given by the modified Halpin–Tsai equation or Lewis–Nielsen equation [32–37]:

$$\frac{P}{P_1} = \frac{1 + AB\phi_2}{1 - B\psi\phi_2} \tag{6}$$

where A is a form factor, $B = ((P_2/P_1) - 1)/((P_2/P_1) + A)$, and $\psi = 1 + (1 - \phi_m/\phi_m^2)\phi_2$. $A = 1.33(L/t)^{0.645}$ when there is no slippage between the matrix and the filler. A will be much smaller if there is slippage.

Another type of composite theory is based on continuous mechanics. If the composite is anisotropic, where the filler has a preferred orientation, the properties of the composite vary with different directions. A Rule of Mixture was easily deduced assuming the direction of measurement is parallel to the orientation of the filler particle:

$$P_L = P_1\phi_1 + P_2\phi_2. \tag{7}$$

In the gelatin–clay nanocomposites, the filler clay platelet is like a flake when in the exfoliated state. The thickness of the single clay platelet is only 1 nm, while the in-plane dimension varies from 20 to 200 nm depending on the type of clay. There are a considerable number of studies of flake-filled composites. It was pointed out that the tensile modulus is close to the value predicted by the Rule of Mixture if the measurement direction is parallel to the plane of flake orientation [31].

The Halpin–Tsai equation and Rule of Mixture were therefore used to predict the properties of gelatin–clay nanocomposites. The Young's modulus of clay nanocrystal is 400 GPa,

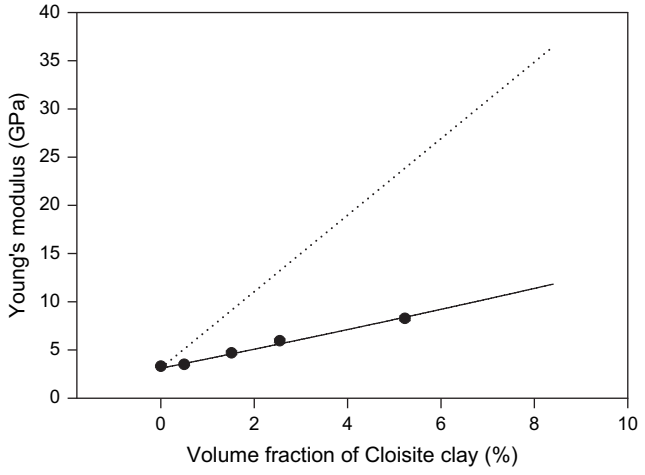

Fig. 7. Young's modulus vs. vol% of clay: experimental data vs. modeling.

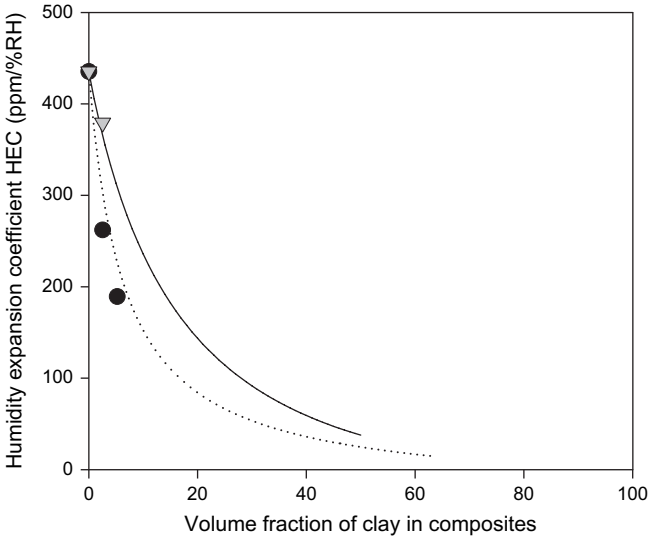

Fig. 8. Comparison of the HEC of gelatin–clay nanocomposite films and that predicted by Eq. (10) based on composite theory. The circle represents gelatin–Cloisite composite films, the triangle represents gelatin–Laponite composite films, the solid line represents the model prediction for a *L*/*t* of 20 and the dashed line represents the model prediction for a *L*/*t* of 200.

which was obtained from molecular dynamic simulation by Manevitch and Rutledge [38]. The density of clay nanocrystal is 2.6 g/cm. Fig. 7 compares the experimental Young's modulus and the predicted value calculated using both the Halpin–Tsai equation and Rule of Mixture of gelatin–Cloisite nanocomposite films. It is shown in Fig. 7 that the predicted Young's modulus using the Halpin–Tsai equation agrees well with the experimental data, while the Rule of Mixture overestimated the value. Therefore, as the Halpin–Tsai equation suggested, the property enhancement is dependent on the interfacial strength between the matrix and nanofiller, the geometry or aspect ratio of the nanoparticle, and the volume fraction of the added nanoparticles. In the case of polymer–clay nanocomposites, strong interfacial strength between polymers and clay nanocrystals, and the exfoliated state, are desirable to improve the Young's modulus and strength of the nanocomposite. The governing principle may be different if the matrix is highly crystalline or if the clay nanoparticles affect the conformation of the polymer chains.

The humidity expansion coefficient is another important property. The treatment can be similar to the thermal expansion coefficient. If the Poisson's ratios of the components are similar, the longitudinal thermal expansion coefficient of a fiber-filled composite is as follows:

$$\alpha_L = \frac{\alpha_1 E_1 \phi_1 + \alpha_2 E_2 \phi_2}{E_1 \phi_1 + E_2 \phi_2} \tag{8}$$

where α is the thermal expansion coefficient and E is the Young's modulus. The humidity expansion coefficient has the same form:

$$\mathrm{HEC}_L = \frac{\mathrm{HEC}_1 E_1 \phi_1 + \mathrm{HEC}_2 E_2 \phi_2}{E_1 \phi_1 + E_2 \phi_2} \tag{9}$$

where HEC is the humidity expansion coefficient.

Eq. (9) can be simplified, assuming HEC_2 is much smaller than HEC_1:

$$\mathrm{HEC}_L = \frac{\mathrm{HEC}_1 E_1 \phi_1}{E_1 \phi_1 + E_2 \phi_2} = \mathrm{HEC}_1 \phi_1 (E_1/E). \tag{10}$$

Shown in Fig. 8, Eq. (10) predicts well the measured humidity expansion coefficients for both gelatin–Laponite and gelatin–Cloisite nanocomposite films. This result suggests that the humidity expansion behavior of the polymer–clay nanocomposite follows the composite theory well when the clay particles are in exfoliated states.

4. Conclusion

In conclusion, high-modulus transparent gelatin–clay nanocomposite films were produced. A large increase in the Young's modulus tensile strength was achieved without sacrificing toughness at a low loading of a montmorillonite type of clay. The humidity expansion coefficient was reduced in the presence of small amounts of clay. XRD illustrates that the clay filler is in an exfoliated state when the clay composition is less than 10 wt%. The addition of clay affects the crystallization of the matrix polymeric material and reduces the crystallinity of the matrix. The Young modulus of the nanocomposite was modeled well using the Halpin–Tsai equation. It revealed that the aspect ratio of the filler, the exfoliation status of clay sheets, the interfacial strength between the matrix and nanoparticles, the dispersion of the clay nanofiller, and the filler content have been shown to have large influences on the properties of nanocomposites.

Acknowledgment

The author greatly appreciates Dr. John Pochan and Dr. Debasis Majumdar for their helpful discussion. Tom Blanton helped with the XRD measurements. The author is also

grateful to Dr. Anthony Dai, Robert Kress, Joe Sedita, and Mario D. Delaura.

References

[1] Usuki A. Mater Sci Eng 1995;C3:109.
[2] Usuki A, Kojima M, Okada A, Fukushima Y, Kurauchi T, Kamigaito O. J Mater Res 1993;8:1179.
[3] Usuki A, Kojima M, Kawasumi M, Okada A, Fukushima Y, Kurauchi T, et al. J Mater Res 1993;8:1185.
[4] Maxfield M, Christiani BR. WO 93/11190 JP; May 1993.
[5] Ke Y, Long C, Qi Z. J Appl Polym Sci 1999;71:1139.
[6] Barbee RB, Matayabas Jr. JC, Gilmer JW. WO 9902593; 1999.
[7] Bagrodia S, Germinario LT, Piner RL, Trexler Jr. JW. WO 9944825; 1999.
[8] Suzuki N. JP 11071509; 1999.
[9] Suzuki N. JP 11323102; 1999.
[10] Toft N, Postoaca I. WO 9950066; 1999.
[11] Akelah AM. J Mater Sci 1996;31:3589.
[12] Noh MW, Lee DC. Polym Bull 1999;42:619.
[13] Giannelis E, Sogah DY, Weimer MW, Chen H. J Am Chem Soc 1999;121:1615.
[14] Lan T, Qian G. Proceedings of additives 2000. Clearwater Beach, FL; Apr 2000.
[15] Hasegawa N, Okamoto H, Kato M, Usuki A, Sato N. JP 11310718; 1999.
[16] Suzuki N. JP 11012451; 1999.
[17] Choi HJ, Kim JW, Kim SG, Jhon MS. Polym Prepr 1999;40:813.
[18] Lan T, Kaviratna PD, Pinnavaia TJ. J Phys Chem Solids 1996;57: 1005.
[19] Doeff MM, Reed JS. Solid State Ionics 1998;113–115:109.
[20] Ivkov R, Gehring PM, Maliszewskyj NC, Krishnamoorti R. Annu Tech Conf – Soc Plast Eng 1999;57:1783.
[21] Aranda P, Ruiz-Hitzky E. Appl Clay Sci 1999;15:119.
[22] Serrano FM, Beall GW, Engman SJ. EP 846723; 1998.
[23] Billingham J, Breen C, Yarwood J. Vib Spectrosc 1997;14:19.
[24] Rao Y, Pochan J. Macromolecules 2007;40:290.
[25] Chem Eng News 1999;38(July).
[26] Waller KE, Marshall AS, Petrie SEB. MTD-R-52-75; 1975.
[27] Bradbury E, Matin C. Proc R Soc 1952;A214:183.
[28] Bradbury E, Matin C. Nature 1951;168:837.
[29] Marshall AS, Petrie SEB. J Photog Sci 1980;28:128.
[30] Shen N, Boyce M, Parks DM, Abes JI, Cohen RE. Polymer 2004;45: 487.
[31] Fornes TD, Paul DR. Polymer 2003;44:4993.
[32] Burgers JM. Second report on viscosity and plasticity. New York: Nordemann; 1938.
[33] Halpin JC. J Compos Mater 1969;3:732.
[34] Ashton JE, Halpin JC, Petit PH. Primer on composite analysis. Lancaster: Technomic; 1969.
[35] Lewis TB, Nielsen LE. J Appl Polym Sci 1970;14:1449.
[36] Nielsen LE. J Appl Phys 1970;41:4626.
[37] Tsai SW, U.S. Govt. Rept. AD 83851; 1968.
[38] Manevitch OL, Rutledge GC. J Phys Chem B 2004;108(4):1428–35.